Title: Suspension and Mixing Characterization of Intermittent Agitation Modes in DASGIP Bioreactors

Authors: Jasmin J Samaras[1], Martina Micheletti[1], Andrea Ducci[2]

Affiliations:[1] Advanced Centre for Biochemical Engineering, University College London, Bernard Katz Building, Gower Street, London, WC1E 6BT, United Kingdom

[2] Department of Mechanical Engineering, University College London, Torrington Place, London, WC1E 7JE, United Kingdom

Corresponding Author: Dr Andrea Ducci, a.ducci@ucl.ac.uk

Abstract:

Intermittent agitation strategies have been increasingly used for a range of process development applications, i.e. to modulate physical cues and improve stem cell differentiation yields and to control hydrodynamic shear stresses in microcarrier suspension, however there is a distinct lack of characterization. This work sought to characterize both continuous and intermittent agitation modes in relation to suspension and mixing dynamics within a DASGIP bioreactor. Suspension dynamics were found to be affected by microcarrier porosity and the degree of settling was found to be more pronounced at the top of the bioreactor. Mixing time characterization showed a marked improvement in mixing efficiency for intermittent agitation, with an overall dependence upon the timing of tracer insertion.

Keywords: Intermittent agitation, mixing dynamics, suspension dynamics

1. Introduction

In recent years, there has been an increasing amount of research into cell cultivation processes based on the use of an intermittent agitation profile over continuous agitation or static culture. In the area of cardiovascular research, Lam *et al.* [1] found that pausing the bioreactor agitation for long time intervals resulted in an improvement of the yield of an embryonic stem cell (ESC) cardiogenic differentiation protocol. The authors postulated that intermittent agitation could be beneficial as it alleviates the agitation-induced necrosis from turbulent eddies, causes a reduction in the number of collisions while enhancing the hydrodynamic physical cues. Studies by Correia *et al.* [2] and Ting *et al.* [3] reported higher yields for a cardiogenic differentiation process when intermittent agitation profiles were adopted. Mechanical forces have historically been proven to modulate cardiogenic differentiation yields as they emulate the cyclic mechanical heartbeat *in vivo*. The authors stipulated that the observed improvement in cardiogenic differentiation efficiency was related to the frequency of mechanical loading generated from the hydrodynamic cues of the intermittent stirring profiles. Other studies have suggested that intermittent agitation may be used during cell culture to promote cell attachment to microcarriers and ensure a homogeneous suspension throughout the bioreactor. Liu *et al.* [4] sought to establish a scalable platform for Vaccinia virus production in CV-1 fibroblast cells. CV-1 cells were attached to Cytodex 1 microcarriers utilizing intermittent agitation for 2 days, before adopting continuous agitation. Fernandes *et al.* [5] employed overnight intermittent agitation regimes during the attachment phase of hESCs to Cytodex 3 microcarriers before setting up continuous agitation for the remaining 15 days of the culture. Dos Santos *et al.* [6] and Nienow *et al.* [7] reported improved microcarrier adherence protocols when utilizing an intermittent agitation strategy during the first few hours post-inoculation.

Intermittent agitation is commonly employed for a range of applications in other industries. For example, Finkler *et al.* [8] demonstrated the beneficial application of intermittent agitation modes in the field of citrus waste biorefining. The use of this agitation mode resulted in minimal substrate agglomeration during the production of pectinases by solid state fermentation, thus improving overall process yield. Tattiyakul *et al.* [9] demonstrated an improvement in heat transfer rates and temperature profiles during a thermal food process when intermittent agitation modes were adopted.

In the aforementioned examples, the impact of intermittent agitation in comparison to continuous and static agitation modes on process yields or process performance is usually

explored and quantified. However, the impact of intermittent agitation has rarely been characterized from an engineering perspective. Flow, mixing and suspension dynamics can be empirically studied to obtain flow patterns, frequency spectra, quality of suspension and mixing efficiency of different bioreactor configurations and operating conditions. Collignon *et al.* [10] investigated the impact of different agitation conditions on the suspension and flow dynamics to inform impeller selection for a microcarrier-based cell cultivation process. Ozturk [11] and Langheinrich and Nienow [12] reported the presence of culture heterogeneities within a stirred bioreactor due to areas of poor mixing which resulted in cell lysis. Flow and mixing dynamics studies by Ducci and Yianneskis [13] and Doulgerakis *et al.* [14] characterized the large-scale vortical structures within a bioreactor and showed the potential for mixing enhancement through amending the feed insertion location. Samaras *et al.* [15] used a frequency analysis approach based on Laser Doppler Anemometry measurements to characterize both continuous and intermittent agitation modes and correlated the flow frequency profiles with the biological outcomes of an induced pluripotent stem cell (iPSC) cardiogenic differentiation protocol. From these observations it is evident that rigorous quantitative analysis is crucial to understand any causal relationship between a change in the hydrodynamic environment and the biological outcome.

The current work is the first to attempt an engineering characterisation of the mixing and suspension dynamics with intermittent agitation. Different dwell strategies are explored within a DASGIP bioreactor and comparisons are made against performance with continuous agitation.

2. Materials and methods

2.1. Bioreactor configuration

A flat-bottomed DASGIP Cellferm-Pro bioreactor system (Eppendorf, Germany) with height, H = 15.5 cm, and diameter, T = 6.2 cm, was equipped with a 6 cm diameter trapezoidal paddle impeller at an off-bottom clearance, C = 1.4 cm (D/T = 0.97, C/T = 0.2). A small temperature probe was also included, located centrally behind the impeller shaft when viewed from the camera point-of-view. A working volume of V_w= 200 mL was used, corresponding to a liquid height, H_L = 6.62 cm. To be able to program the impeller rotational speed (i.e. continuous and intermittent modes) the magnetically driven impeller commonly installed in DASGIP bioreactors was replaced by top-driven configuration, with the shaft attached to a fully programmable N-Series Allen Bradley Motor unit. The system was mounted within a water

filled glass trough, and a NET iCube camera (NET, Germany) connected to an adjustable arm was used to acquire sets of images at increasing speeds for different agitation strategies. A white LED panel was installed behind the reactor to minimize background noise and maximize visualization.

2.2. Suspension characterization

Two types of commercially available microcarriers, Cultispher-G (ρ = 1.04 g mL^{-1}, average particle diameter, D_{50} = 255 μm, D = 130-380 μm and porosity, $\Phi \approx$ 50% with pore size 10–30 μm, Percell Biolytica, Sweden) and Cytopore 1 (ρ = 1.03 g mL^{-1}, D_{50} = 235 μm, D = 200-270 μm, $\Phi >$ 90% with pore size 30 μm, GE Healthcare, USA) were used in these experiments. Cultispher-G is made from a Gelatin matrix whilst Cytopore 1 is made up of a cross-linked cellulose matrix, substituted with positively charged N,N-diethylaminoethyl (DEAE) groups. Similar to the work of Olmos *et al.* [16] the microcarriers were stained using 0.4% Trypan Blue (Sigma-Aldrich, USA) and experiments were conducted at a concentration of 1 g L^{-1} using MilliQ water with pH 6.998. The experimental protocol was designed to assess suspension at increasing speeds with the microcarriers completely settled on the bottom of the reactor at the beginning of each experiment (i.e. stationary impeller). Images were then recorded at a frequency of 2 Hz for 5 minutes per condition. This allowed experimental data both during the transient and the steady-state phases of the suspension process and acquire enough images in the steady-state to reliably establish the degree of suspension. Continuous impeller agitation was performed at N = 10–200 rpm, whilst intermittent agitation was investigated at N = 90 rpm, with motion stopped every 30 s (T_{inv} = 30 s) for a duration of 30 s (T_{dwell} = 30 s). Images were processed using a purposely-written MATLAB code where the homogenous suspension index, H, defined in Eq. (1) was used:

$$H = 1 - \frac{(I_N - I_{max})}{(I_0 - I_{max})} \quad (1)$$

Where I_N is the cumulative brightness of the image at speed, N, I_0 represents the image brightness when the system is stationary and fully settled and I_{max} denotes when the system is completely suspended. Conditions of full suspension were associated to $H \geq$95%.

2.3. Mixing dynamics

Mixing time characterization was conducted using the Dual Indicator System for Mixing Time (DISMT), first described by Melton *et al.* [17]. DISMT is based upon a fast acid-base reaction between NaOH and HCl, monitored with the addition of two pH indicators, Methyl Red and

Thymol Blue. Methyl Red is red under acidic conditions, turning yellow once pH 5.6 and above is reached. Thymol Blue is blue under basic conditions, turning yellow at pH 8.0 and below. Both indicators show yellow in the neutral pH range of 5.6–8.0.

Stock solutions of the two indicators were added to MilliQ water at a concentration of 4.67 mL L^{-1} Thymol Blue and 4.26 mL L^{-1} of Methyl Red. 200 mL of the prepared DISMT solution was then added to the bioreactor and 15 μL of 0.75 M HCl was inserted and fully mixed. Impeller agitation was initiated at the rotational speed or agitation mode under investigation and image acquisition was initiated. A stoichiometric amount of 0.75 M NaOH was then added and images were acquired at a frame rate of 2 Hz for 5 minutes at each experimental condition to ensure the 'steady state' was achieved. Continuous agitation modes were investigated at N = 75, 90, 105 and 120 rpm. Intermittent agitation modes were investigated at N = 90 rpm, T_{inv} = 30 s and T_{dwell} = 500–30000 ms. Five repeats per condition were completed. Images were then post-processed using a purposely-written MATLAB code, where the mixing time was determined from the standard deviation of the normalized image green channel over time (further detail available in [18]).

3. Results and discussion

3.1. Suspension characterization

The first part of this study aimed at characterizing the changes in suspension dynamics between continuous and intermittent agitation modes. As highlighted in the introduction, intermittent agitation is commonly employed in a number of bioprocess applications such as enhancing cell seeding and detachment from microcarriers [5-7] as well as promoting stem cell differentiation [2]. In this section suspension dynamics have been investigated for two commercially available microcarrier types, Cultispher-G and Cytopore 1 (see Sect. 2.2 for details).

The variation in time of the degree of homogenous suspension in 9 locations across the reactor for a fixed rotational speed N = 70 rpm, is given Figs. 1A and 1B for Cultispher-G and Cytopore 1, respectively. The curves are color-coded to the corresponding region shown in the figure inset. From Fig. 1A (Cultispher-G) it is evident that the transient - initial suspension gradient - and the steady state plateau are highly dependent on the region considered within the reactor. As expected, regions closer to the bottom of the reactor are subject to faster rates of suspension, the steepest gradients occurring in regions 1-3 and achieving complete suspension within seconds from the start of the experiment. In moving higher up the tank a lower steady state degree of suspension is reached. For example, region 8 at the top-center of the reactor is always

below the 90% threshold. In general, suspension takes place symmetrically with regions next to the reactor walls being denoted by similar curves, while the center region for each elevation considered is shown to suspend slower. The exception is region 2, which is predominantly masked in the image post-processing due to the impeller position and therefore cannot be considered as representative of the local suspension process. It can be concluded that for the DASGIP bioreactor suspension occurs most rapidly at the sides of the tank, where a radial jet generated by the paddle impinges against the wall and is redirected in the axial directions.

→Insert Figure 1←

Considering Cytopore 1 (Fig. 1B), which represents microcarriers of similar size and density to Cultispher-G, but with a significant higher porosity (Φ > 90%), it is apparent that much faster suspension is achieved at the same rotational speed, i.e. 70 rpm. The plateau of each region is achieved ≈10 s earlier than for the Cultispher-G and there is much less variance in the degree of suspension achieved between the different regions. The outermost regions suspend comparably to the corresponding center region at each height and the plateau in all cases reaches 99–100% homogeneity. A zoomed in view of the transition phase is given in the inset where some oscillation in the curves is apparent. This is most evident in the top regions closer to the bioreactor walls (regions 7 and 9), which display a frequency of ≈0.87 Hz. Similar oscillations were observed for other rotational speeds and depending on the range of speed considered two non-dimensional frequency, f/N, were found: f/N = 0.81 ± 0.06 for N = 30–80 rpm and f/N = 0.48 ± 0.04 for N = 90–200 rpm. These oscillations are not present in the Cultispher-G experiments and might be related to the interaction of the axial velocity fluctuations induced by impeller motion next to the reactor wall and the high degree of porosity of Cytopore 1.

The steady state degree of suspension, H, achieved by each region at increasing speed, N = 10–200 rpm, is plotted in Figs. 2A and 2B for Cultispher-G and Cytopore 1, respectively. The speed to full suspension, N_H, is determined when H = 95%. In agreement with the curves of Fig. 1A, Fig. 2A (Cultispher-G) confirm that suspension is achieved most efficiently at the bioreactor walls. This effect becomes more pronounced towards the top of the tank. The uppermost center region 8 requires a rotational speed of approximately 85.4 rpm to be considered fully suspended. In comparison, regions 7 and 9 can be considered fully suspended at 73.7 rpm. Regions 4 and 6 are characterized by full homogenous suspension at 53.9 rpm, which indicate the suspension process along the reactor elevation is gradual for microcarriers of intermediate porosity ($\Phi \approx 50\%$).

→Insert Figure 2←

Fig. 2B shows very little difference between the regions considered when Cytopore 1 microcarriers are used. For example, the homogenous suspension speed, N_H for regions at the bottom wall of the reactor is 28.9 rpm (regions 1 and 3) while N_H = 29.8 rpm at the top-central region (region 8). Overall, it can be concluded that microcarriers of larger porosity (Cytopore 1) suspend faster and reach a nearly homogenous concentration across the reactor almost instantaneously. Intermediate porosity microcarriers, such as Cultispher-G, are subject to more gradual suspension.

Operating under intermittent agitation modes, the resulting suspension profile clearly portrays the stop in impeller motion, as indicated in Fig. 3. Comparison is made between Cultispher-G (Fig. 3A) and Cytopore 1 (Fig. 3B), where it can be observed that the drop in suspension increases significantly for lower microcarrier porosity (Fig. 3A), there may also be some affect due to Cytopore 1 surface charge that must be further investigated. Similar to the analyses carried out for continuous agitation, the degree of microcarrier settling has been assessed in 9 regions across the reactor. It is interesting to note that the microcarriers have not completely settled during the relatively long dwell time of 30 s. The degree of suspension, however, is approximately 10% in the regions closer to the top of the vessel, while values around 50% are retained within the central part of the reactor. In agreement with the suspension experiments shown in Fig. 1A, regions in proximity to the bioreactor walls are also the quickest to be affected by the stop in impeller motion. This suggests the presence of a strong circulation loop induced by impeller motion up the bioreactor wall, which is rapidly lost once motion is halted. Despite the difference in settling, resuspension is rapid and all regions resume suspension values within a few seconds from the restart of the impeller.

→Insert Figure 3←

Cytopore 1 microcarriers are less affected by the impeller stoppage with the degree of suspension remaining greater than 60% over the 30 s of dwell in the entire reactor (Fig. 3B). When comparing the data of regions 7 and 9 it seems that the settling rate is more pronounced on the left side of the reactor. This asymmetry could be attributed to the presence of a single temperature probe present behind the impeller as seen from the camera point of view (*cf* Fig. 3B). Considering the impeller rotation is from right-to-left, the left-side of the reactor is subject to a drop in velocity due to the flow obstruction of the probe. This aspect is more pronounced during the dwell.

3.2. Mixing dynamics

The second stage of our study sought to characterize mixing dynamics during both continuous and intermittent agitation modes. As in the previous section, the characterization was first performed for continuous agitation (Fig. 4). A plot of the measured standard deviation over time for five separate experimental repeats at N = 90 rpm is given in Fig. 4A, where the mixing process starts at the instant of feed insertion, t = 0. The peak standard deviation represents full dispersion of the tracer and corresponds to the instant when the reactor displays the largest variety of hues. The decrease in standard deviation then represents the mixing process to the 'fully mixed' steady state. When considering the five experimental repeats, there is a clear distinction between the dispersion process of repeats 1-3 and 4-5. The dispersion time, t_D, for repeats 1-3 is relatively quick, 4.95 ± 0.25 s, with corresponding mixing time, of t_m=16.65 ± 1.95 s, whilst for experimental repeats 4 and 5 these time scales are significantly larger, t_D = 11.95 ± 0.83 s and t_m = 42.2 ± 7.7 s, respectively. To ascertain the cause for this discrepancy the instant of feed insertion was observed for each experimental repeat (Fig. 4B). The feed blob is encircled for each experimental repeat. Despite the insertion process being made through the same port hole in the reactor headplate, it is clear that for repeats 1-3 the blob is consistently inserted deeper into the bioreactor volume, while in repeats 4 and 5 the basic addition is entrained at the liquid surface, further from the impeller. This explains the significantly longer dispersion times in repeats 4 and 5 and the large standard deviation.

→Insert Figure 4←

Mixing dynamics were characterized for a range of rotational speeds deemed appropriate for cell culture applications, N = 75–120 rpm. Experimental repeats were considered separately depending upon tracer insertion to above or below $z/H_L \approx 0.65$. Fig. 4C presents the characterized mixing times for each speed. When insertion is made closer to the impeller region mixing occurs more rapidly and with less variation. This suggests that to improve consistency in the mixing process and reduce mixing time, feed insertion in the DASGIP reactor must reach a certain depth ($z/H_L \approx 0.65$). The mixing number, Nt_m, associated to the lower tracer insertion conditions plateaus between N = 90–120 rpm, $Nt_m \approx 21.9 \pm 2$, suggesting a turbulent flow regime is achieved.

The variation of mixing time with dwell time during intermittent agitation is presented in Fig. 5. To consistently compare with the data obtained for continuous agitation, only experiments with depth of insertion at or below $z/H_L \approx 0.65$ are represented. The data have been divided

into two subsets, depending on the timing of tracer insertion with respect to the dwell: within 4 s from the end of dwell, denoted as “close to the end of dwell” and more than 4 s from the end of the dwell, denoted as “in between dwells”. As a reference the mixing time determined for continuous agitation at N = 90 rpm is included in Fig. 5 (t_m = 15.98 s). Overall, the introduction of intermittent agitation has improved the mixing efficiency with shorter mixing times being observed. For shorter dwell durations, little distinction can be seen in mixing time with respect to the timing of tracer addition. For $T_{dwell} \geq 9000$ ms the timing of the tracer addition is shown to become more influential towards mixing performance. The improvement in mixing efficiency might be attributable to the high shear generated at the restart of the impeller, which is more pronounced the longer fluid momentum is lost during the dwell. A "close to the end of dwell" strategy takes full advantage of this mechanism as time spent during dwell (no motion) by the inserted dye in the reactor is minimal. On the contrary, when insertion of the tracer is made "in between dwells" the mixing time is shown to steadily increase and full advantage of the shear generated at the impeller restart is not taken. It is noteworthy that standard deviation of "close to the end of dwell" experiments is low, indicating high repeatability.

→Insert Figure 5←

4. Conclusions

The suspension dynamics in the DASGIP bioreactor were found to be significantly affected by the microcarrier porosity. During intermittent agitation the degree of suspension of Cultispher-G in the top part of the reactor was found to decrease to 10% for a dwell time of 30 s, the degree of suspension for Cytopore 1 remained above 60% in the entire reactor. In general, the settling rate was found to be constant and therefore the degree of settling for different dwell times can be extrapolated from the current data. For both continuous and intermittent agitation modes the wall regions displayed higher rates of suspension and settling. This suggests the presence of a strong circulation loop up at the bioreactor wall during impeller motion which is rapidly lost when the impeller is stationary. Further characterization of the flow dynamics would help elucidate the flow patterns.

The mixing characterization studies showed the importance of tracer depth before dispersion and the impact this can have upon mixing efficiency and repeatability. When tracer was inserted lower within the bioreactor faster and more repeatable mixing times were achieved. The introduction of intermittent agitation yielded an improvement in mixing efficiency which

might be related to the high shear generated at the impeller restart. The extent of improvement of mixing efficiency depends on dwell duration and tracer insertion strategies adopted. "Close to the end of dwell" strategies are favourable as they take advantage of the high shear generated at impeller restart, with mixing times 30% lower than continuous agitation, showing high repeatability.

Future work in this space seeks to further explore the hydrodynamics and suspension characteristics under different agitation modes to define suitable dimensionless parameters and scale invariants, thus supporting process development studies in cell-based product applications.

5. Acknowledgements

This work was supported by the Centre for Doctoral Training (CDT) in Innovative Manufacturing in Emerging Macromolecular Therapies, Engineering and Physical Sciences Research Council (EPSRC) [EP/L015218/1] and by the European Union's Horizon 2020 research and innovation programme [grant agreement No: 739572].

Symbols used

Symbols

C	[m]	Impeller clearance
D	[m]	Impeller diameter
D_{50}	[m]	Median particle diameter
f	[Hz]	Frequency
H	[m]	Tank height
$H_{(N)}$	[%]	Homogeneity index at speed N
H_L	[m]	Liquid height
N	[s^{-1}]	Rotational speed
N_H	[s^{-1}]	Minimum speed to homogeneity
Nt_m	[-]	Mixing number
T	[m]	Tank diameter
t_D	[s]	Dispersion time
T_{dwell}	[s]	Dwell time or duration of impeller stoppage
T_{inv}	[s]	Interval time of impeller motion
t_m	[s]	Mixing time
V_w	[L]	Working fluid volume

Greek letters

Φ	[%]	Porosity
ρ	[g cm^{-3}]	Density
σ	[-]	Standard deviation

Abbreviations

DISMT	Dual Indicator System for Mixing Time
ESC	Embryonic Stem Cell
iPSC	Induced Pluripotent Stem Cell

References

[1] A. T. L. Lam, A. K. L. Chen, J. Li, W. R. Birch, S. Reuveny, S. K. W. Oh, *Stem Cell Res. Ther*. **2014**, 5 (5), 110-125. DOI: 10.1186/scrt498

[2] C. Correia, M. Serra, N. Espinha, M. Sousa, C. Brito, K. Burkert, Y. Zheng, J. Hescheler, M. J. T. Carrondo, T. Sarić, P. M. Alves, *Stem Cell Rev.* **2014**, 10 (6), 786-801. DOI: 10.1007/s12015-014-9533-0

[3] S. Ting, A. Chen, S. Reuveny, S. Oh, *Stem Cell Res.* **2014**, 13 (2), 202-213. DOI: 10.1016/j.scr.2014.06.002

[4] S. Liu, L. Ruban, Y. Wang, Y. Zhou, D. N. Nesbeth, *Heliyon*. **2017**, 3 (2), 1-20, DOI: 10.1016/j.heliyon.2017.e00238

[5] A. M. Fernandes, P. A. N. Marinho, R. C. Sartore, B. S. Paulsen, R. M. Mariante, L. R. Castilho, S. K. Rehen, *Brazilian J. Med. Biol. Res.* **2009**, 42 (6), 515-522. DOI: 10.1590/S0100-879X2009000600007

[6] F. Dos Santos, P. Z. Andrade, G. Eibes, C. L. da Silva, J. M. S. Cabral, *Methods Mol. Biol.* **2011**, 698, 189-198. DOI: 10.1007/978-1-60761-999-4_15

[7] A. W. Nienow, C. J. Hewitt, T. R. J. Heathman, V. A. M. Glyn, G. N. Fonte, M. P. Hanga, K. Coopman, Q. A. Rafiq, *Biochem. Eng. J.* **2016**, 108, 24-29. DOI: 10.1016/j.bej.2015.08.003

[8] A. T. J. Finkler, A. Biz, L. O. Pitol, B. S. Medina, H. Luithardt, L. F. Luz, N. Krieger, D. A. Mitchell, *Biochem. Eng. J.* **2017**, 121, 1-12. DOI: 10.1016/j.bej.2017.01.011

[9] J. Tattiyakul, M. A. Rao, A. K. Datta, *J. Food Eng.* **2002**, 54 (4), 321-329. DOI: 10.1205/096030802753479070

[10] M. L. Collignon, A. Delafosse, M. Crine, D. Toye, *Chem. Eng. Sci.* **2010**, 65 (22), 5929-5941. DOI: 10.1016/j.ces.2010.08.027

[11] S. S. Ozturk, *Cytotechnology*. **1996**, 22, 3-16. DOI: 10.1007/BF00353919

[12] C. Langheinrich, A. W. Nienow, *Biotechnol. Bioeng.* **1999**, 66 (3), 171-179. DOI: 10.1002/(SICI)1097-0290(1999)66:33.0.CO;2-T

[13] A. Ducci, M. Yianneskis, *AIChE J.* **2007**, 53 (2), 305-315. DOI: 10.1002/aic.11076

[14] Z. Doulgerakis, M. Yianneskis, A. Ducci, *Chem. Eng. Res. Des.* **2009**, 87 (4), 412-420. DOI: 10.1016/j.cherd.2008.12.019

[15] J. J. Samaras, B. Abecasis, M. Serra, A. Ducci, M. Micheletti, *J. Biotechnol.* **2018**, 287, 18-27. DOI: 10.1016/j.cherd.2008.12.019

[16] E. Olmos, K. Loubiere, C. Martin, G. Delaplace, A. Marc, *Chem. Eng. Sci.* **2015**, 122, 545-554. DOI: 10.1016/j.ces.2014.08.063

[17] L. A. Melton, C. W. Lipp, R. W. Spradling, K. A. Paulson, *Chem. Eng. Commun.* **2002**, 189 (3), 322-338. DOI: 10.1080/00986440212077

[18] G. Rodriguez, W. Weheliye, T. Anderlei, M. Micheletti, M. Yianneskis, A. Ducci, *Chem. Eng. Res. Des.* **2013**, 91 (11), 2084-2097. DOI: 10.1016/j.cherd.2013.03.005

Figure captions

Figure 1: Variation in time of the degree of microcarriers suspension in the 9 regions denoted in the inset at a fixed rotational speed, N = 70 rpm : (A) Cultispher-G; (B) Cytopore 1.

Figure 2: Variation of the 'steady state' degree of suspension in the 9 regions denoted in the inset for increasing rotational speeds, N = 10–200 rpm: (A) Cultispher-G; (B) Cytopore 1.

Figure 3: Suspension in segregated regions over time for intermittent agitation conditions, N = 90 rpm, T_{inv} = 30 s and T_{dwell} = 30,000 ms: (A) Cultispher-G; (B) Cytopore 1.

Figure 4: Continuous agitation mixing analysis: (A) Progression of mixing over time for 5 experimental repeats at N = 90 rpm; (B) Tracer blob location before dispersion; (C) Mixing time according to tracer blob height before dispersion.

Figure 5: Intermittent agitation mixing analysis, segregated according to tracer addition close to the end of the dwell and in between dwells (> 4 s) at N = 90 rpm, T_{inv} = 30 s and T_{dwell} = 500–30,000ms.

Type of Article:
Intermittent agitation although commonly used in a range of applications is yet to undergo any engineering characterization in the literature. This study introduces the characterization of both continuous and intermittent agitation modes within bioreactor configuration, focusing upon the impact of microcarrier suspension dynamics and culture mixing efficiency.

Suspension and mixing characterization of continuous and intermittent agitation modes

J. Samaras, M. Micheletti, A. Ducci

Chem. Eng. Technol. **2019**, *XX (X)*,
xxxx…xxxx

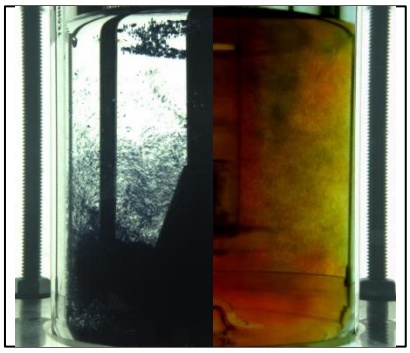

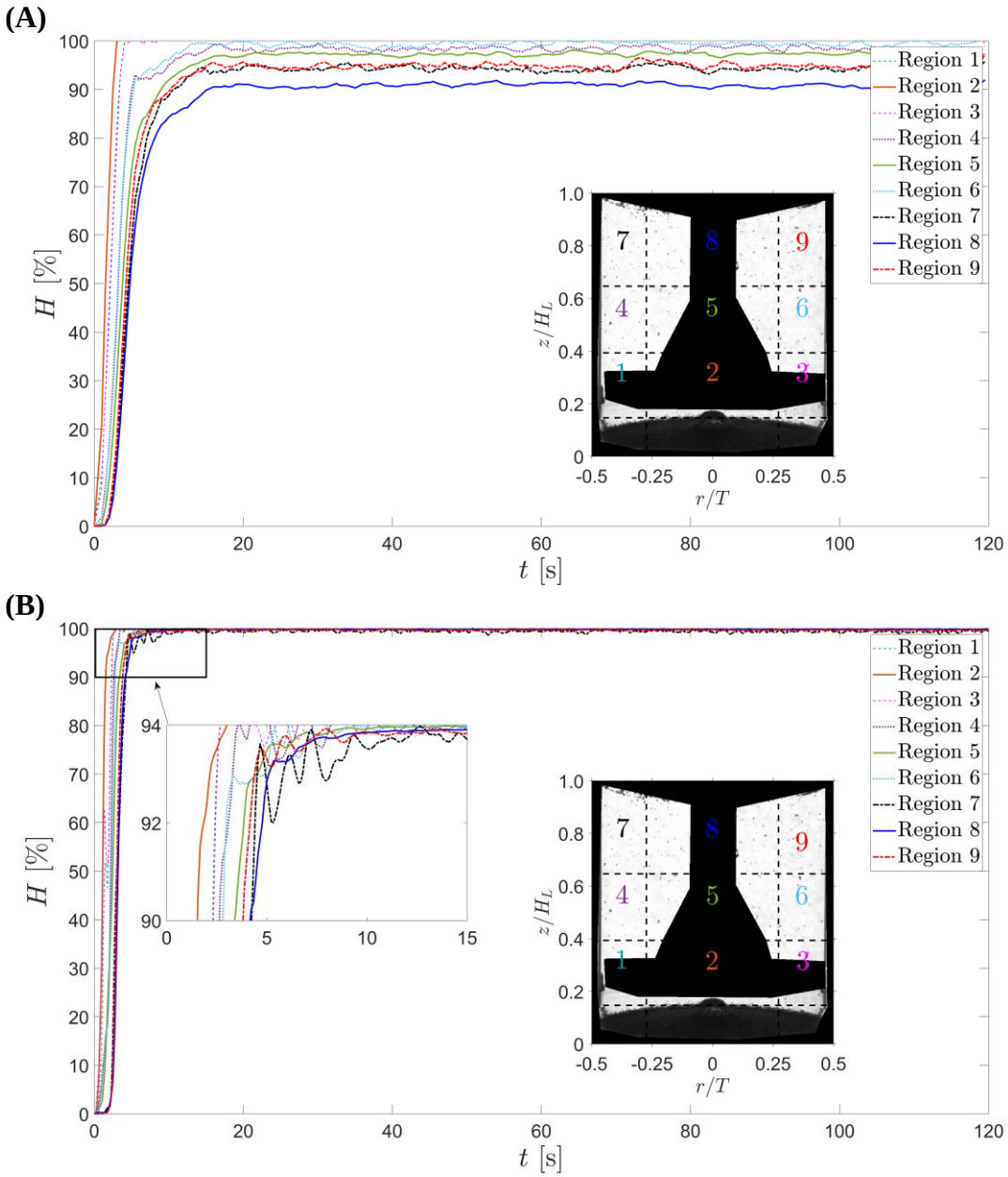
(A)
(B)
H [%]
t [s]
z/H_L
r/T
Region 1
Region 2
Region 3
Region 4
Region 5
Region 6
Region 7
Region 8
Region 9

Figure 1

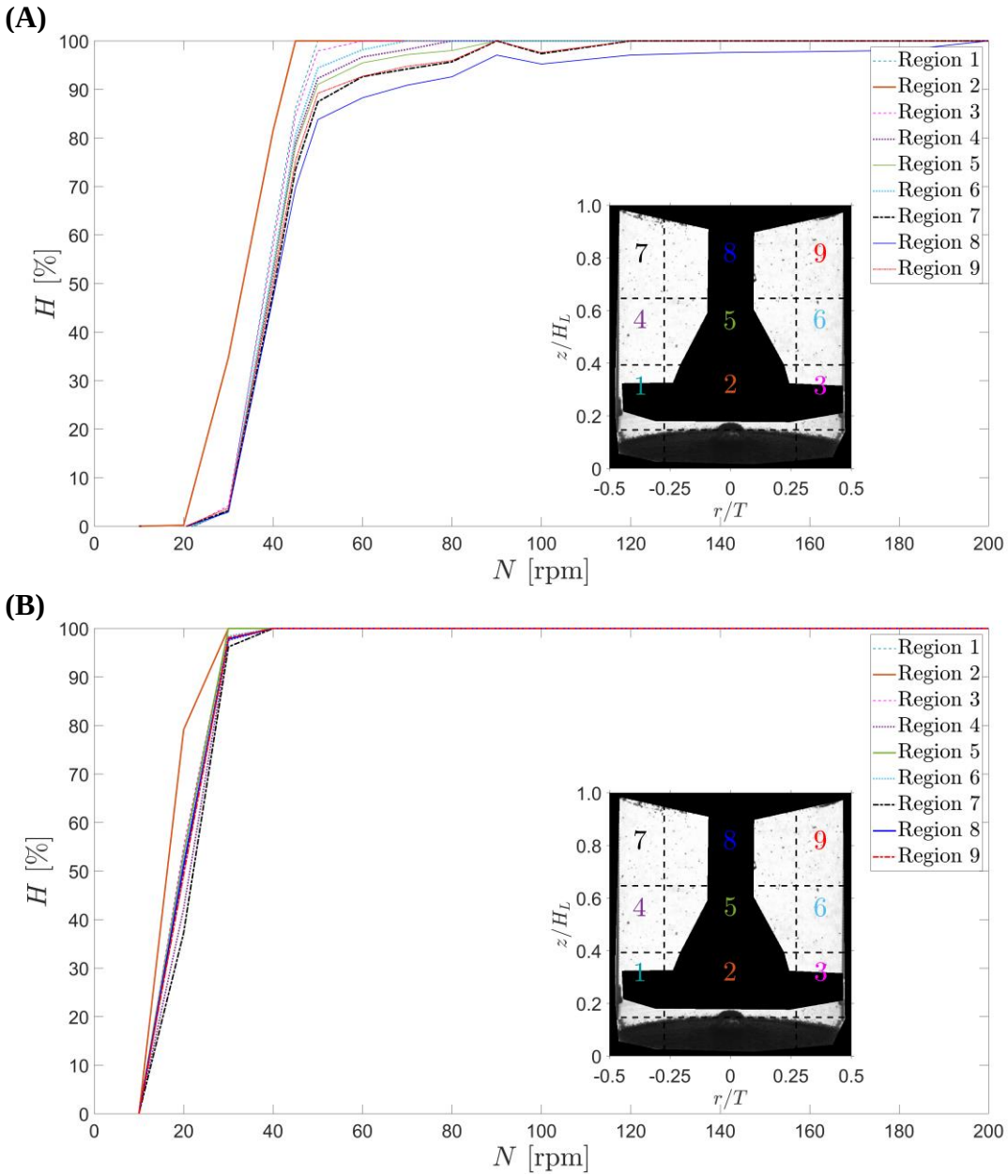
(A)
H [%]
N [rpm]
Region 1
Region 2
Region 3
Region 4
Region 5
Region 6
Region 7
Region 8
Region 9
z/H_L
r/T
(B)
H [%]
N [rpm]
Region 1
Region 2
Region 3
Region 4
Region 5
Region 6
Region 7
Region 8
Region 9
z/H_L
r/T

Figure 2

(A)

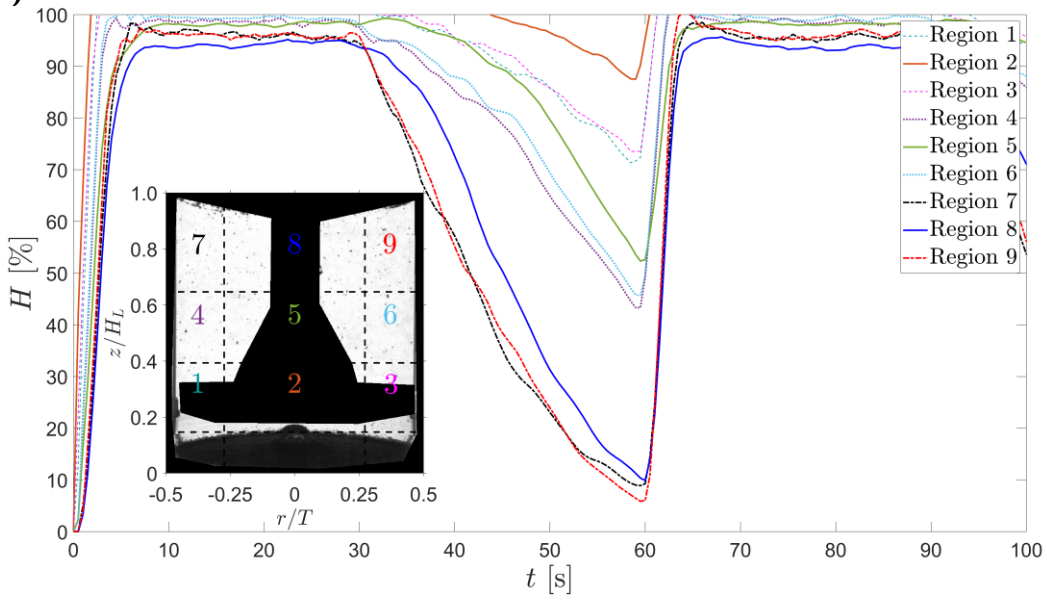
H [%]
t [s]
Region 1
Region 2
Region 3
Region 4
Region 5
Region 6
Region 7
Region 8
Region 9
z/H_L
r/T
7
8
9
4
5
6
1
2
3

(B)

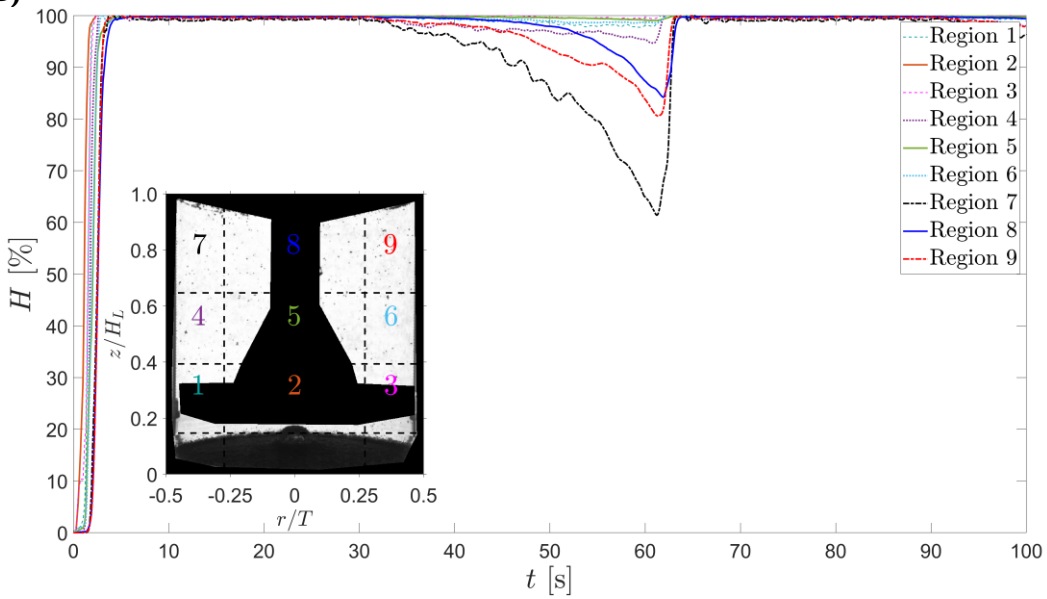
H [%]
t [s]
Region 1
Region 2
Region 3
Region 4
Region 5
Region 6
Region 7
Region 8
Region 9
z/H_L
r/T
7
8
9
4
5
6
1
2
3

Figure 3

(A)

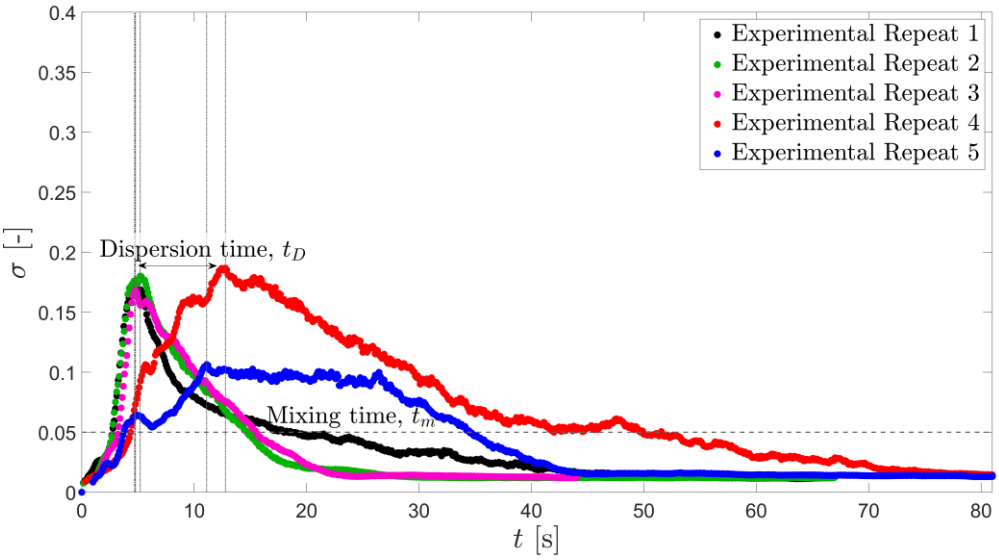

(B)

Experimental Repeats 1 - 3	Experimental Reapeats 4 & 5
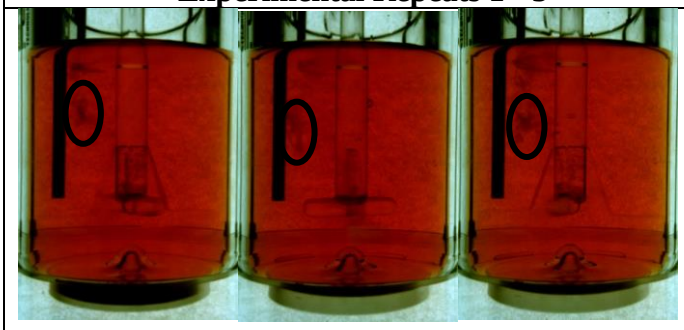	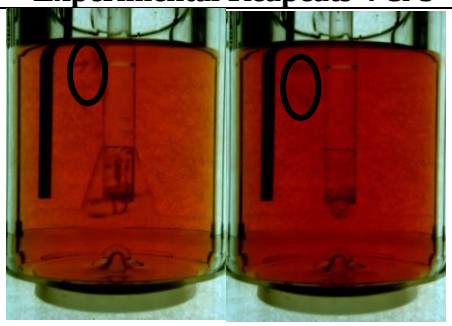

(C)

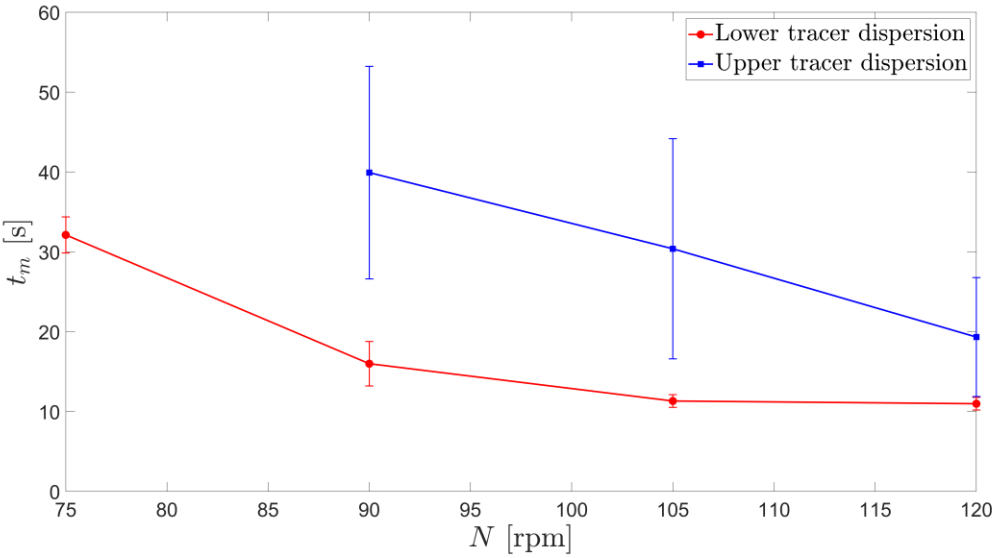

Figure 4

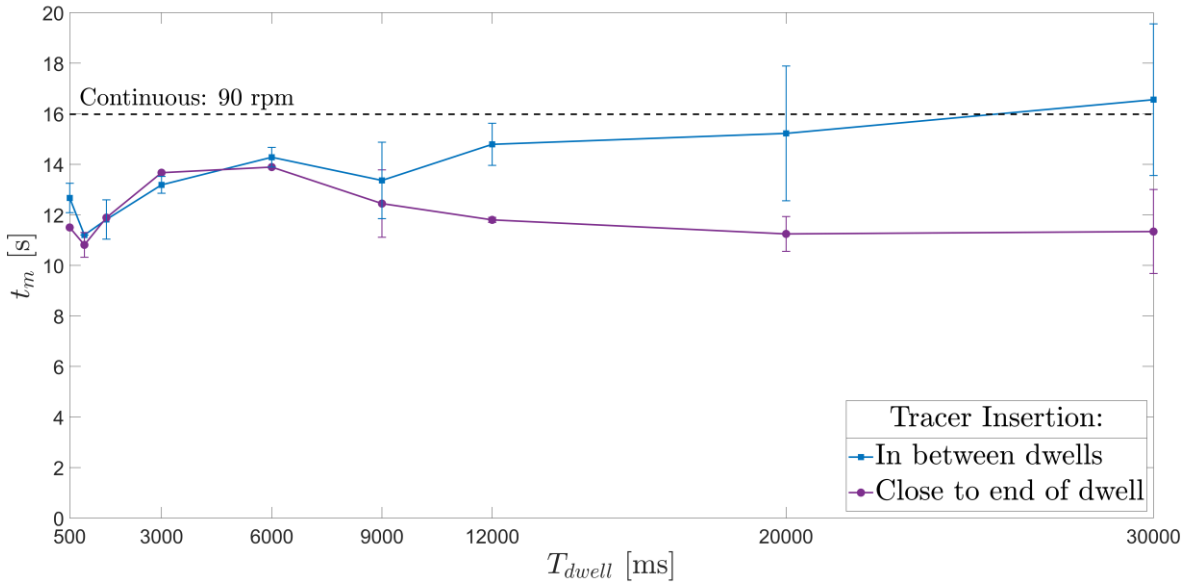
Continuous: 90 rpm
t_m [s]
T_{dwell} [ms]
Tracer Insertion:
In between dwells
Close to end of dwell
0
2
4
6
8
10
12
14
16
18
20
500
3000
6000
9000
12000
20000
30000

Figure 5